Free Radical Research, April 2011; 45(4): 417–430

informa
healthcare

EPR detection of cellular and mitochondrial superoxide using cyclic hydroxylamines

SERGEY I. DIKALOV[1], IGOR A. KIRILYUK[2], MAXIM VOINOV[3] & IGOR A. GRIGOR'EV[2]

[1]*FRIMCORE, Emory University School of Medicine, Atlanta, GA, USA,* [2]*Novosibirsk Institute of Organic Chemistry, Novosibirsk, Russia, and* [3]*North Carolina State University, Raleigh, NC, USA*

(Received date: 2 July 2010; In revised form date: 10 November 2010)

Abstract

Superoxide ($O_2^{\bullet-}$) has been implicated in the pathogenesis of many human diseases, but detection of the $O_2^{\bullet-}$ radicals in biological systems is limited due to inefficiency of $O_2^{\bullet-}$ spin trapping and lack of site-specific information. This work studied production of extracellular, intracellular and mitochondrial $O_2^{\bullet-}$ in neutrophils, cultured endothelial cells and isolated mitochondria using a new set of cationic, anionic and neutral hydroxylamine spin probes with various lipophilicity and cell permeability. Cyclic hydroxylamines rapidly react with $O_2^{\bullet-}$, producing stable nitroxides and allowing site-specific $O_2^{\bullet-}$ detection in intracellular, extracellular and mitochondrial compartments. Negatively charged 1-hydroxy-4-phosphono-oxy-2,2,6,6-tetramethylpiperidine (PP-H) and positively charged 1-hydroxy-2,2,6,6-tetramethylpiperidin-4-yl-trimethylammonium (CAT1-H) detected only extramitochondrial $O_2^{\bullet-}$. Inhibition of EPR signal by SOD2 over-expression showed that mitochondria targeted mitoTEMPO-H detected intramitochondrial $O_2^{\bullet-}$ both in isolated mitochondria and intact cells. Both 1-hydroxy-3-carboxy-2,2,5,5-tetramethylpyrrolidine (CP-H) and 1-hydroxy-3-methoxycarbonyl-2,2,5,5-tetramethylpyrrolidine (CM-H) detected an increase in cytoplasm $O_2^{\bullet-}$ stimulated by PMA, but only CM-H and mitoTEMPO-H showed an increase in rotenone-induced mitochondrial $O_2^{\bullet-}$. These data show that a new set of hydroxylamine spin probes provide unique information about site-specific production of the $O_2^{\bullet-}$ radical in extracellular or intracellular compartments, cytoplasm or mitochondria.

Keywords: *Superoxide, spin trap, cyclic hydroxylamine, intracellular, extracellular, EPR*

Introduction

Superoxide radical ($O_2^{\bullet-}$) is one of the most important free radicals both in chemistry and biology [1]. It is produced by one-electron reduction of oxygen and frequently a precursor of other reactive oxygen species (ROS) such as hydrogen peroxide (H_2O_2), peroxynitrite ($ONOO^-$), lipid and hydroxyl radicals [2]. In biological systems $O_2^{\bullet-}$ plays a dual role: under physiological conditions $O_2^{\bullet-}$ is involved in cell signalling [3] and in pathophysiological states over-production of $O_2^{\bullet-}$ leads to oxidative stress causing cellular dysfunction and cell death [4]. Pathological conditions such as hypertension, atherosclerosis and hypercholesterolemia are strongly associated with increased $O_2^{\bullet-}$ production [5]. Nonetheless, measurements of $O_2^{\bullet-}$ in biological samples is still a challenging task due to limitations of existing techniques for $O_2^{\bullet-}$ detection [6] and the diversity of the sources of $O_2^{\bullet-}$ production [7].

The most commonly used chemiluminescence technique for measurement of $O_2^{\bullet-}$ is lucigenin-enhanced chemiluminescence [6]. The validity of this technique, however, has been questioned on the grounds that $O_2^{\bullet-}$ production might be artificially over-estimated because of a phenomenon known as redox cycling, in which the lucigenin radical can react with oxygen to generate $O_2^{\bullet-}$ [8].

Reduction of ferricytochrome c by $O_2^{\bullet-}$ to ferrocytochrome c was frequently used in the past for $O_2^{\bullet-}$ detection [6]. Unfortunately, this spectrophotometric detection was limited to extracellular $O_2^{\bullet-}$ because cytochrome c is not cell permeable and it did lack sensitivity and specificity due to reduction of ferricytochrome c

Correspondence: Sergey Dikalov, PhD, FRIMCORE Director, Division of Cardiology, Emory University School of Medicine, 1639 Pierce Drive, Atlanta, GA 30322, USA. Tel: 404-712-9550. Fax: 404-727-3585. Email: dikalov@emory.edu

ISSN 1071-5762 print/ISSN 1029-2470 online
DOI: 10.3109/10715762.2010.540242

by electrons donated from enzymes and other molecules.

One of the most definitive methods of $O_2^{\bullet-}$ identification is electron paramagnetic resonance (EPR) spectroscopy [9,10]. The EPR spin-trapping technique has been used to detect short-lived $O_2^{\bullet-}$ radicals by following the formation of persistent radical adducts. Theoretically, spin trapping should be an ideal way to detect radicals in biological tissues. Unfortunately, this turns out not to be the case. First, nitrone spin traps react with $O_2^{\bullet-}$ very slowly ($k \sim 35–75\ M^{-1}s^{-1}$, pH = 7.4) [11], limiting spin trapping to only extracellular $O_2^{\bullet-}$ because spin traps cannot compete with intracellular antioxidants, rapidly reacting with $O_2^{\bullet-}$ ($k \sim 10^5–10^9\ M^{-1}s^{-1}$) [12]. Second, $O_2^{\bullet-}$ radical adducts are unstable and undergo decomposition to $^{\bullet}OH$-radical adducts [13–15] or reduction to EPR-silent products by ascorbate, transition metal ions or flavin-enzymes [14]. These limitations make the spin trapping technique useful for identification and qualitative analysis but not suitable for quantification of intracellular $O_2^{\bullet-}$.

Because of the aforementioned problems with nitrone spin traps, investigators have turned their attention to other molecules such as dihydroethidium for $O_2^{\bullet-}$ detection in biological samples [6,16]. The dihydroethidium method, however, has several problems. It is a light-sensitive compound which is also prone to auto-oxidation. Dihydroethidium requires a two-step reaction in order to detect $O_2^{\bullet-}$, which involves free radical intermediate [17]. Furthermore, formation of '$O_2^{\bullet-}$-specific' product can be affected by peroxidase reactions, which may compromise specificity of the assay [18].

We have previously reported that cyclic hydroxylamines can be used for measurement of $O_2^{\bullet-}$ in cultured cells, tissues and *in vivo* [19,20]. These molecules are not spin traps, they do not 'trap' radicals, but they are oxidized with $O_2^{\bullet-}$ to form EPR-detectable stable nitroxides with half-lives of several hours in cell cultures. Since both spin traps and cyclic hydroxylamines generate species detectable by EPR we suggest to name these cyclic hydroxylamines as 'hydroxylamine spin probes' which must not be confused with nitroxide spin probes. Cyclic hydroxylamines react with $O_2^{\bullet-}$ much faster ($k \sim 10^3–10^4\ M^{-1}s^{-1}$, pH = 7.4) compared to nitrone spin traps and can compete with cellular antioxidants for intracellular $O_2^{\bullet-}$ [11]. Due to high efficiency in detection of $O_2^{\bullet-}$ radical hydroxylamine, probes can be used at very low concentrations (0.05–1 mM) compared to spin traps (10–50 mM), which minimizes side-effects of the probes on the biological samples. Cyclic hydroxylamine detect the $O_2^{\bullet-}$ radical in a single chemical reaction, while other probes like dihydroethidium and lucigenin require at least two reactions, which may cause artifacts [17]. In contrast to lucigenin or 2',7'-dichlorofluorescin, hydroxylamine probes are not engaged in redox cycling and therefore they allow us to avoid problems with artificial $O_2^{\bullet-}$ production [21]. It is also important to note that the potential competition between hydroxylamine and nitroxide [22] does not affect the $O_2^{\bullet-}$-mediated oxidation of hydroxylamine because the hydroxylamine/nitroxide ratio is usually very high [11].

Several cyclic hydroxylamines, such as 1-hydroxy-3-carboxy-2,2,5,5-tetramethylpyrrolidine (CP-H) [23,24], 1-hydroxy-3-methoxycarbonyl-2,2,5,5-tetramethylpyrrolidine (CM-H) [19,20,23–27], 1-hydroxy-4-phosphono-oxy-2,2,6,6-tetramethylpiperidine (PP-H) [11,28,29] and 1-hydroxy-2,2,6,6-tetramethylpiperidin-4-yl-trimethylammonium chloride (CAT1-H) [30] (Figure 1) were successfully used for detection and quantitative measurements of $O_2^{\bullet-}$ in cultured cells and tissue samples. Some of these cyclic hydroxylamine probes have been successfully applied not only *ex vivo* but also *in vivo* [6,20]. Hydroxylamine probes can be potentially oxidized by several ROS and, therefore, to define the contribution of specific ROS it is necessary to perform control experiments with supplementation of superoxide dismutase (SOD), peroxynitrite scavenger urate or other scavengers [26,31,32]. For example, we have found that in cultured cells or isolated vessels PEG-SOD lowers the EPR signal by more than 70% [19].

Despite significant progress in applications of hydroxylamine probes, investigation of $O_2^{\bullet-}$ production in different sub-cellular compartments is still a challenging problem. The aim of this work was to investigate site-specific $O_2^{\bullet-}$ production in different cellular compartments using a new set of cationic, anionic and neutral hydroxylamine spin probes (Figure 1) with various lipophilicity and cell permeability. For this purpose we have investigated $O_2^{\bullet-}$ production in a cell-free xanthine oxidase system, mitochondria, neutrophils and endothelial cells. Efficiency of $O_2^{\bullet-}$ detection was compared with the nitrone spin trap 5-ethoxycarbonyl-5-methyl-1-pyrroline N-oxide (EMPO).

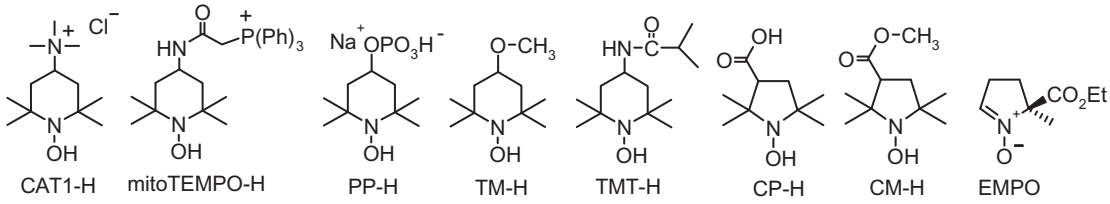

Figure 1. Chemical structures of hydroxylamine spin probes and the spin trap EMPO.

Cell permeability and lipophilicity of various cyclic hydroxylamines were measured. This new set of probes has demonstrated site-specific measurement of $O_2^{\bullet-}$ in extracellular or intracellular compartments, cytoplasm or mitochondria.

Materials and methods

Cyclic hydroxylamines 1-hydroxy-2,2,6,6-tetramethylpiperidin-4-yl-trimethylammonium chloride (CAT1-H), 1-hydroxy-3-carboxy-2,2,5,5-tetramethylpyrrolidine hydrochloride (CP-H), 1-hydroxy-3-methoxycarbonyl-2,2,5,5-tetramethylpyrrolidine (CM-H), 1-hydroxy-4-phosphono-oxy-2,2,6,6-tetramethylpiperidine (PP-H), 1-hydroxy-4-methoxy-2,2,6,6-tetramethylpiperidine (TM-H), N-(1-Hydroxy-2,2,6,6-tetramethylpiperidin-4-yl)-2-methylpropanamide (TMT-H), 1-hydroxy-4-[2-(triphenylphosphonio)-acetamido]-2,2,6,6-tetramethylpiperidine (mitoTEMPO-H,), spin trap 5-ethoxycarbonyl-5-methyl-1-pyrroline N-oxide (EMPO) and 3-morpholinosydnonimine (SIN-1) were purchased from Enzo Life Sciences (San Diego, CA). Polyethylene glycol-conjugated superoxide dismutase (PEG-SOD), phorbol 12-myristate 13-acetate (PMA) and all other reagents were obtained from Sigma-Aldrich (St. Louis, MO). Stock solutions of cyclic hydroxylamines (10 mM) were prepared in argon-purged 0.9% NaCl treated with 25 g/L Chelex-100 and containing 50 μM desferoxamine or 0.1 mM DTPA. Stock solutions were kept under argon on ice and were prepared daily.

Cell culture and mitochondria isolation

Bovine aortic endothelial cells (BAEC, passage 4–8) were cultured on 100 mm plates in Media 199 containing 10% foetal calf serum supplemented with 2 mM L-glutamine and 1% vitamins. Confluent cells were used for the experiments [26]. Human aortic endothelial cells (HAEC) were purchased from Lonza (Chicago, IL) and cultured in EGM-2 medium supplemented with 2% FBS, but without antibiotics. On the day before the study, the FBS concentration was reduced to 1%. HAEC were transfected with GFP or SOD2 plasmid was described previously [31]. Rat aortic smooth muscle cells were purchased from Cell Systems (Kirkland, Wash). Neutrophils were isolated from whole blood by Percoll density gradient centrifugation as previously described [33].

Brain mitochondria were isolated from the male Lewis rat pooled forebrain. We used the modified method of Sims [34] to isolate and purify brain mitochondria (RBM) in a Percoll gradient. Endothelial mitochondria were isolated using the digitonin method as previously described [35].

All animal use complied with National Institutes of Health guidelines and was approved by the Emory University Institutional Animal Care and Use Committee [36].

Superoxide measurement

The cell-free xanthine oxidase superoxide-generating system contained xanthine oxidase (1 mU/ml), xanthine (50 μM) and DTPA (0.1 mM) in 50 mM sodium phosphate buffer (pH = 7.4) containing 0.9% NaCl [37].

Measurement of mitochondrial $O_2^{\bullet-}$ was performed in media containing 125 mM KCl, 10 mM MOPS, 2 mM $MgSO_4$, 2 mM KH_2PO_4, 10 mM NaCl, 1 mM EGTA and 0.7 mM $CaCl_2$, 50 μM desferoxamine, pH = 7.2. Mitochondrial $O_2^{\bullet-}$ production was studied in the presence of 2 mM malate + 20 mM glutamate and 20 μg of mitochondrial protein [29]. The amount of detected $O_2^{\bullet-}$ was calculated from inhibition of EPR signal with 50 U/ml Cu,Zn-SOD. All mitochondria measurements were carried out at 25°C using a Bruker EMX spectrometer equipped with a Temperature Controller system.

Neutrophils were incubated with 1 mM of corresponding cyclic hydroxylamine and stimulated by the addition of 1 μM PMA in Chelex-treated phosphate buffer, pH = 7.4 [27].

Production of $O_2^{\bullet-}$ in bovine aortic endothelial cells (BAEC) was measured in Krebs–Hepes buffer (KHB) containing 5.786 g/L NaCl, 0.35 g/L KCl, 0.368 g/L $CaCl_2$, 0.296 g/L $MgSO_4$, 2.1 g/L $NaHCO_3$, 0.142 g/L K_2HPO_4, 5.206 g/L Na-Hepes, 2 g/L D-glucose, pH = 7.35, in the presence of 25 μM desferoxamine and 2.5 μM diethyldithiocarbamate. Cellular production of $O_2^{\bullet-}$ was stimulated by mitochondrial inhibitor antimycin A (5 μM) [16,29] or pre-treatment of cells with peroxynitrite donor SIN-1 [26]. Confluent endothelial cells were treated with 1 mM SIN-1 for 60 min at 37°C and then washed with PBS. Superoxide production was analysed in cell suspensions incubated at room temperature with hydroxylamine spin probes (1 mM) or the spin trap EMPO (50 mM). The rate of $O_2^{\bullet-}$ formation was in xanthine oxidase system, mitochondria, neutrophils or BAEC was measured by monitoring the amplitude of the low-field component of the EPR spectrum as previously described [11]. The concentration of nitroxide was determined from a calibration curve for intensity of the EPR signal of 3-carboxyproxyl at various known concentrations. The rate of $O_2^{\bullet-}$ production was calculated from the accumulation of nitroxide, obtained from the EPR time scan. For this purpose, the EPR kinetics were analysed using linear regression and WinEPR software (Bruker Biospin Corp, Billerica, MA). EPR settings were as follows: modulation amplitude, 2 G; microwave power, 20 mW; conversion time, 1.3 s; time constant, 5.2 s. Samples were scanned immediately after supplementation of spin probes unless stated otherwise.

Production of intracellular $O_2^{\bullet-}$ in intact human aortic endothelial cells (HAEC) was stimulated with PMA (5 μM, 30 min). Generation of mitochondrial $O_2^{\bullet-}$ was induced by rotenone (5 μM, 30 min).

Following treatment with PMA, rotenone or vehicle, HAEC were incubated with 0.5 mM spin probes for 20 min at 37°C. Then cells were collected and placed into a 1 ml syringe with 0.6 ml buffer and the suspension was snap-frozen in liquid nitrogen. Samples were analysed in finger Dewar vessel filled with liquid nitrogen [6]. ESR spectra were recorded using the following ESR settings: field sweep, 80 G; microwave frequency, 9.39 GHz; microwave power, 2 mW; modulation amplitude, 5 G; conversion time, 327.68 ms; time constant, 5242.88 ms; 512 points resolution and receiver gain, 1×10^4.

Analysis of cell permeability of hydroxylamine probes

Cell permeability of hydroxylamine probes was determined in cellular lysates. For this purpose confluent rat aortic smooth muscle cells were subjected to 20-min incubation with corresponding hydroxylamine (1 mM) at 37°C. Then cells were centrifuged and supernatant discarded. Cells were resuspended in PBS and lysated by ultrasound. Spin probe cellular content was determined by oxidation of cell lysates with $NaIO_4$ (50 mM) to convert cyclic hydroxylamines into nitroxides detected by EPR [38].

To determine partition coefficients, solutions of the hydroxylamines (1 mM) in 50 mM phosphate buffer saline (pH 7.4) were prepared. The portions of the solutions were extracted with an equal amount of octanol. The concentrations of hydroxylamine probes in water phase were calculated from EPR intensities of samples treated with $NaIO_4$ (50 mM) to convert cyclic hydroxylamines into nitroxides. The partition coefficients were determined from a ratio of hydroxylamine concentrations in the phosphate buffer before (I_0) and after (I) a single extraction with an equal amount of octanol, $K_p = (I_0/I) - 1$. EPR measurements were performed in 50 µL glass capillary tubes at room temperature using the Bruker EMX spectrometer. Spectrometer settings were as follows: field sweep, 60 G; microwave frequency, 9.82 GHz; microwave power, 20 mW; modulation amplitude, 1 G; conversion time, 164 ms; time constant 328 ms; sweep time, 168 s; receiver gain, 1×10^5; number of scans, 4.

Results

Reaction of hydroxylamine spin probes with $O_2^{\bullet-}$

All the hydroxylamine spin probes readily reacted with $O_2^{\bullet-}$ produced in a cell-free xanthine oxidase system [37]. Figure 2 demonstrates comparison of $O_2^{\bullet-}$ detection using the spin trap EMPO (50 mM) and the spin probe TMT-H (1 mM). Spin trapping of $O_2^{\bullet-}$ by EMPO produced the relatively stable EMPO/$^{\bullet}$OOH radical adduct with the characteristic six-line EPR spectrum (Figure 2A, insert). The accumulation of EMPO/$^{\bullet}$OOH radical adduct was monitored by following the intensity of the low-field component of its EPR spectrum. The rate of accumulation of the radical adduct (130 nM/min) decreased by more than 60% after 6-min data acquisition (Figure 2A, XO+X). Addition of Cu,Zn-SOD (50 U/ml) to xanthine/xanthine oxidase completely blocked the accumulation of the radical adduct (Figure 2A, XO+X+SOD).

Reaction of TMT-H with $O_2^{\bullet-}$ produced the stable nitroxide radical 4-isobutyramido-TEMPO (TMT), which has a three-line EPR spectrum (Figure 2B, insert). Addition of Cu,Zn-SOD (50 U/ml) to the reaction mixture blocked nitroxide accumulation

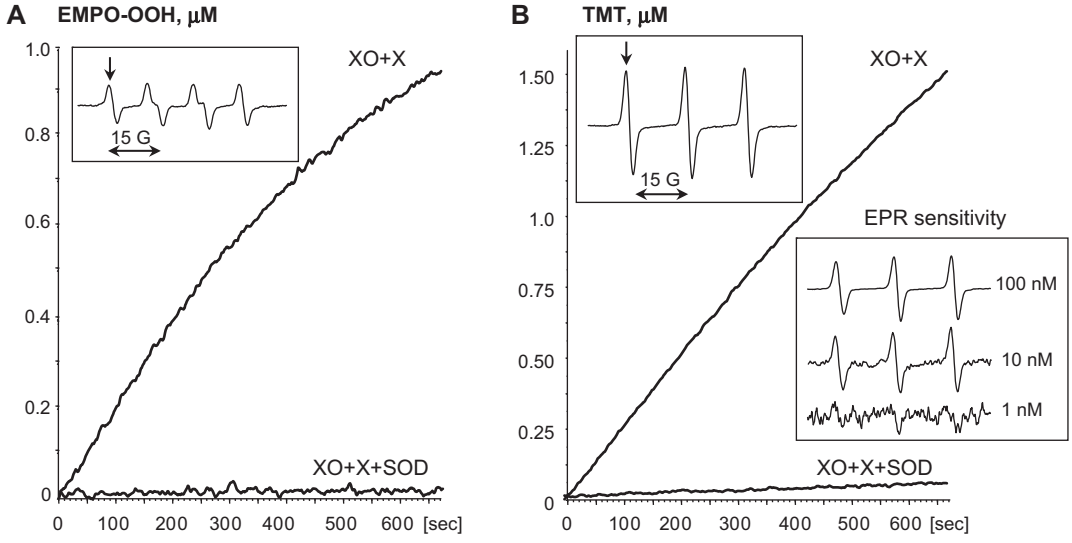

Figure 2. EPR detection of the nitroxides formed from the spin trap EMPO (A) and the hydroxylamine spin probe TMT-H (B) in a xanthine oxidase $O2^{\bullet-}$ generating system (XO+X, 1 mU/ml xanthine oxidase plus 50 µM xanthine). Graphs show typical time scans of nitroxide accumulation followed by low field component of EPR spectrum (insert). Analysis of EPR sensitivity shows that Bruker EMX spectrometer equipped with SHQ microwave cavity has a detection limit of 1 nM nitroxide.

(Figure 2B, XO+X+SOD). Interestingly, there was no significant difference in the initial rates of accumulation of the EMPO/•OOH and TMT, but after 6-min the difference in the rates of product accumulation was more than 2-fold (Figure 2). As a result, concentration of TMT was more than 60% higher than concentration of EMPO/•OOH after the 11 min scan, which is likely due to the lower stability of the EMPO/•OOH radical adduct compared to TMT nitroxide.

Other cyclic hydroxylamine probes (CAT1-H, PP-H, CP-H and CM-H) showed similar accumulation of nitroxides in the xanthine oxidase system and supplementation of SOD blocked accumulation of nitroxides in a dose-dependent manner (Figure 3), while catalase did not affect kinetics of nitroxide production (data not shown). Competition of SOD and hydroxylamines was used to measure the rate constant of the spin probe reaction with $O_2^{\bullet-}$. Figure 3 shows the linear graphs of $V/V_0 - 1$ (where V and V_0 represent the rates of nitroxide accumulation in the presence or absence of SOD, respectively) as a function of SOD activity, as was previously described [23,39]. The slope of the graph reflects the ratio of k_{SOD}/k_{Probe}, therefore, higher slope corresponds to lower rate constant. Among the hydroxylamines studied, the positively charged mitoTEMPO-H and CAT1-H show the highest rate constants of reaction with $O_2^{\bullet-}$, while the negatively charged PP-H shows the smallest rate constant. The ratio of the slopes equals the ratio of the apparent reaction rate constants of corresponding hydroxylamine spin probes with superoxide. Taking into account the value of the rate constant for the reaction of CP-H with $O_2^{\bullet-}$ reported earlier (3.2×10^3 $M^{-1}s^{-1}$) [23] the corresponding rate constants for TM-H, TMT-H, CM-H, mitoTEMPO-H and CAT1-H were estimated (Table I). The reactivity of $HO_2^{\bullet-}$ is known to be higher than that of $O_2^{\bullet-}$ [39]. Moreover, cyclic hydroxylamines are known to be bases, with pK varying in a broad range (5–8), depending on electronic and steric effects of the substituents, and the reactivity of free hydroxylamine base may differ strongly from that of hydroxylammonium cation [40]. Therefore, the apparent reaction rates of the hydroxylamine probes with $O_2^{\bullet-}/HO_2^{\bullet}$ are expected to demonstrate complex pH-dependence, which deserves a separate study. Finally, it is important to note that correct determination of 'absolute values' for the reaction rate constants from competition kinetics using biological sources of superoxide may be complicated. Therefore, the apparent rate constants presented in Table I should be taken primarily for the ranking purpose and considered as a semi-quantitative.

Lipophilicity and cell permeability of spin probes

Cell permeability of the spin probes may affect the outcome of the cellular $O_2^{\bullet-}$ detection. Lipophilicity is an important factor modulating cellular permeability of the cyclic hydroxylamines and the partition coefficient in a water/octanol mixture is a standard measure of lipophilicity. The partition coefficients of the spin probes were determined in octanol/phosphate buffer saline at pH = 7.4 mixture as octanol/aqueous phase concentration ratio. Relatively high lipophilicity of CM-H, TMT-H and TM-H (Table I) is an indication of their ability to cross cell membranes.

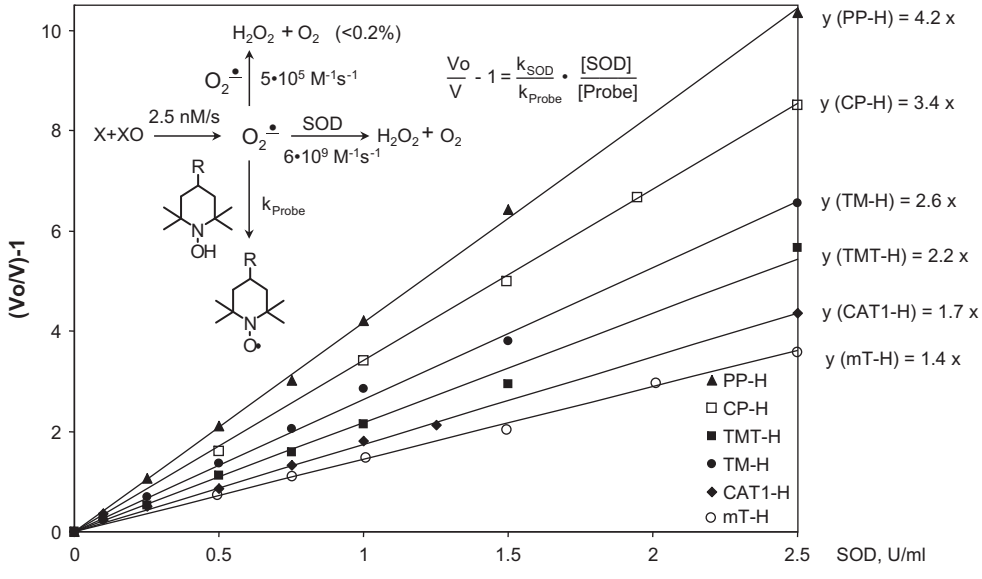

Figure 3. Reaction of hydroxylamine spin probe with O2•− and measurement of the rate constants by competition with SOD. Superoxide radicals were produced by xanthine (50 μM) plus xanthine oxidase (1 mU/ml). The rate constants were calculated from inhibition of nitroxide formation at various SOD activities using the following equation: $(V_0/V) - 1 = k_{SOD} \times [SOD]/k_{Probe} \times [Probe]$, where V_0 and V represent the rates of nitroxide formation in the absence or presence of SOD, respectively. The k_{Probe} and k_{SOD} are the second order rate constants of the $O_2^{\bullet-}$ reactions with spin probes and SOD. The slope of the graph reflects the ratio of k_{SOD}/k_{Probe}. Higher slope corresponds to lower rate constant.

Table I. Partition coefficients (K_p) of cyclic hydroxylamines, rate constants of their reactions with $O_2^{\bullet-}$ and rates of nitroxide accumulation in PMA-stimulated neutrophils[a], in BAEC[b] under basal conditions and after treatment with peroxynitrite donor SIN-1.

	CAT1-H	PP-H	CP-H	CM-H	TMT-H	TM-H	mT-H	EMPO
K_p	0.001	0.005	0.05	27	35	43	8	
$k(O_2^{\bullet})$, $\times 10^{-3}$ $M^{-1}s^{-1}$	6.4 ± 0.4	0.84 [28]	3.2 [23]	12 [6]	4.9 ± 0.5	4.2 ± 0.4	7.8 ± 0.6	0.074 [9]
[a]Neutrophils + PMA, nM/min	936 ± 28	929 ± 35		1153 ± 52		932 ± 31		562 ± 25
[b]BAEC, nM/min	12 ± 1	20 ± 3		95 ± 5	15 ± 2	14 ± 2		12 ± 2
[b]BAEC+SIN-1, nM/min	22 ± 2	60 ± 5		122 ± 6	41 ± 3	38 ± 4		21 ± 2

[a]for experiment details see Figure 5; [b]for experiment details see Figure 6.

Low lipophilicity of CP-H most likely results from ionization of the carboxylic group (pK_a is ca. 5) at physiological pH values. However, ionization of the carboxylic group only attenuates the cell permeability but does not abolish it completely. Ionic PP-H and CAT1-H showed the lowest lipophilicity.

We studied cell permeability of the hydroxylamine spin probes in cultured rat aortic smooth muscle cells. For this purpose rat aortic smooth muscle cells were subjected to 20-min incubation with corresponding hydroxylamine probe. Then cells were centrifuged and cellular content of the probe was determined by oxidation of cell lysates with $NaIO_4$ (50 mM) to convert cyclic hydroxylamines into nitroxides detected by EPR [38]. We found that CM-H, PP-H, TM-H and TMT-H accumulated in the cellular cytoplasm (Figures 4A–E). No significant accumulation of CAT1-H in the cells was observed (Figure 4F).

Lipophylic triphenylphosphonium cation is known to be cell-permeable and provide mitochondria-targeted accumulation [41]. Indeed, incubation of cells with 50 μM mitochondria-targeted spin probe mitoTEMPO-H resulted in significant cellular accumulation of mitoTEMPO (Figure 4C). The concentration of mitoTEMPO in cellular lysate was close to nitroxide concentration in lysates of cells incubated with 1 mM TM-H or TMT-H, thereby supporting active cellular accumulation of mitoTEMPO-H. Indeed, mitochondria isolated from mitoTEMPO-H treated cells showed strong EPR spectra (data not shown).

It has been previously been suggested that hydrophilic nitroxides do not diffuse through cellular lipid membranes. The absence of cell permeability for CAT1-H is in line with this assumption. However, PP-H unexpectedly demonstrates high capacity of cellular accumulation similar to neutral CM-H. Our data (Figure 4) suggest that cells actively import PP-H through some unknown mechanism. The mechanism of PP-H accumulation by cells could be similar to the active transport of phosphate [42]. This process is ATP-dependent and mitochondrial uncoupling should inhibit accumulation of PP-H. Indeed, we found that accumulation of PP-nitroxide in vascular cells was inhibited by antimycin A and PP-nitroxide was not accumulated in red blood cells which are deficient of mitochondria (data not shown).

Detection of extracellular $O_2^{\bullet-}$ in human neutrophils

Previously, we have shown that human neutrophils produce predominantly extracellular $O_2^{\bullet-}$, both in basal and PMA-stimulated conditions [27]. In this work we compared $O_2^{\bullet-}$ detection by spin probes and the spin trap EMPO in human neutrophil suspensions. Production of $O_2^{\bullet-}$ was monitored by accumulation of nitroxides or EMPO radical adducts which were followed by the increase in the low-field component of their EPR spectra. The rate of nitroxide accumulation significantly increased upon stimulation of neutrophils with PMA. Specificity of $O_2^{\bullet-}$ detection by spin probes was confirmed by inhibition of EPR signal with SOD supplementation (Figure 5). The rate of CM-H oxidation into nitroxide was 20% higher than that of spin probes PP-H, TM-H and CAT1-H, while accumulation of the EMPO radical adduct was

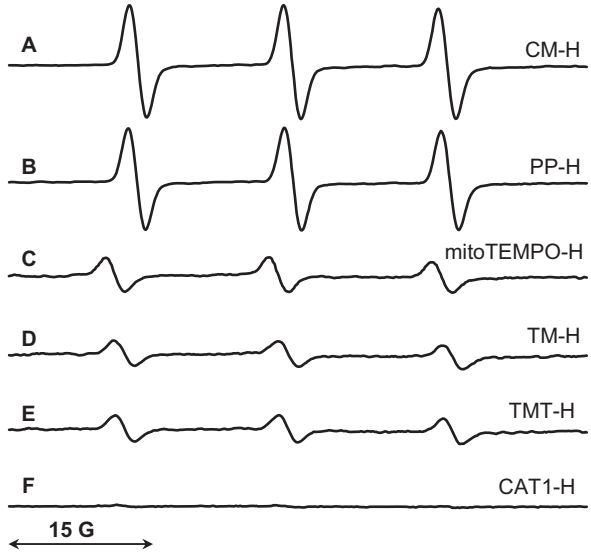

Figure 4. Cell permeability of hydroxylamine spin probes. Confluent rat aortic smooth muscle cells were incubated with 1 mM cyclic hydroxylamines (50 μM mitoTEMPO-H) for 20 min at 37°C. Cell lysate was treated with 10 mM $NaIO_4$ before EPR measurements. The figure shows typical EPR spectra observed in at least three independent experiments.

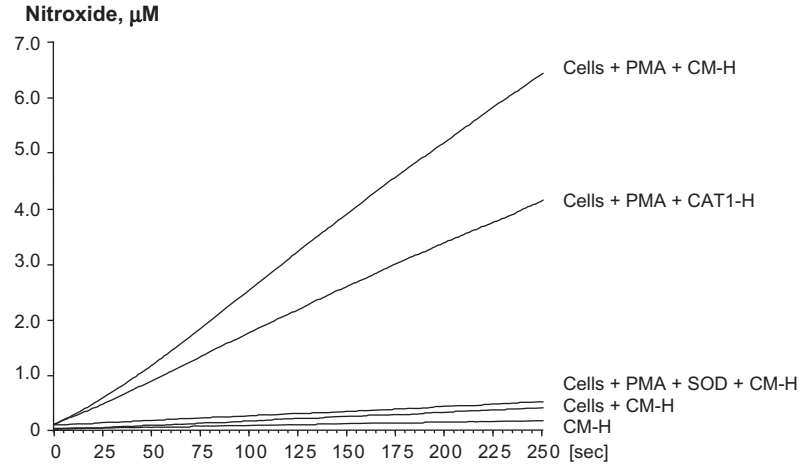

Figure 5. Superoxide production was by PMA-stimulated human neutrophils (0.15 mg/ml). Cells were stimulated by 1 μM phorbol 12-myristate 13-acetate (PMA) and incubated with 1 mM hydroxylamine probes or 50 mM EMPO.

2-fold lower than nitroxide formation from the spin probes (Figure 5, Table I). These differences in $O_2^{\bullet-}$ detection in PMA-stimulated neutrophils correlated with the cell-free experiments in a xanthine oxidase $O_2^{\bullet-}$ generating system (Figures 3 and 5).

Detection of $O_2^{\bullet-}$ in intact endothelial cells treated with the peroxynitrite donor SIN-1

It has been previously reported that that exposure of endothelial cells to peroxynitrite leads to oxidation of tetrahydrobiopterin (BH_4), which is a crucial intracellular cofactor of eNOS (Figure 6, Scheme) [43]. Depletion of cellular BH_4 results in uncoupling of endothelial NO synthase (eNOS), which then produce $O_2^{\bullet-}$ instead of NO [25,43]. Nitric oxide synthase inhibitor L-NAME blocks $O_2^{\bullet-}$ production by uncoupled eNOS [25,43,44], which is likely due to inhibition of heme domain of eNOS [45]. Uncoupling of eNOS by peroxynitrite donor SIN-1 is a well-known model of endothelial dysfunction which increases both intra- and extra-cellular $O_2^{\bullet-}$ production in endothelial cells [25,26]. We have investigated production of endothelial $O_2^{\bullet-}$ after eNOS uncoupling using hydroxylamine probes and the spin trap EMPO.

Both EMPO and the hydroxylamine probes detected $O_2^{\bullet-}$ produced by BAEC (Figure 6, Table I). Interestingly, CAT1-H and EMPO formed similar amounts of nitroxides. The nitroxides formation from CAT1-H and EMPO was completely suppressed by Cu,Zn-SOD supplementation; thus, it corresponds to basal extracellular production of $O_2^{\bullet-}$. Reactions with other spin probes gave stronger EPR signals and supplementation with extracellular SOD did not inhibit nitroxide accumulation completely. Presumably, CM-H, PP-H, TM-H and TMT-H react with intracellular $O_2^{\bullet-}$. CM-H showed highest reactivity among hydroxylamine spin probes producing the highest amount of nitroxide (Figure 6, Table I).

Uncoupling of eNOS was induced by 1-h incubation of endothelial cells with 1 mM peroxynitrite donor SIN-1, the later was then washed out with PBS

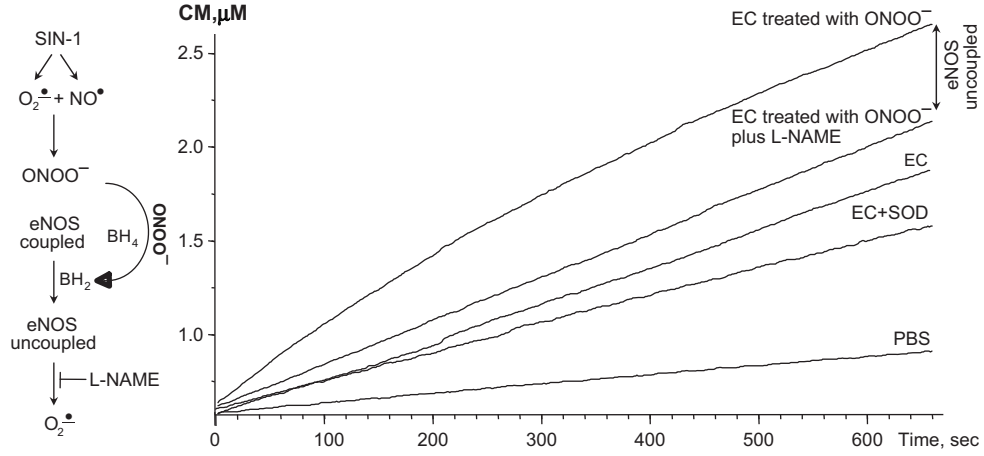

Figure 6. Intra- and extracellular O2$^{\bullet-}$ production in bovine aortic endothelial cells (BAEC) treated with the peroxynitrite donor SIN-1. Confluent endothelial cells were treated with 1 mM SIN-1 for 60 min at 37°C, then washed with PBS. Superoxide production was analysed in cell suspensions incubated at room temperature with hydroxylamine spin probes (1 mM) or the spin trap EMPO (50 mM).

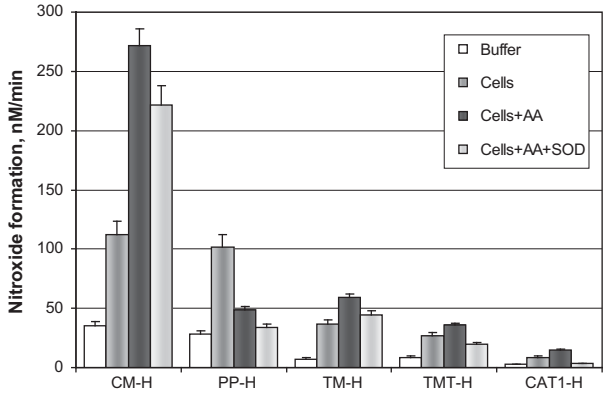

Figure 7. Detection of intra- and extracellular mitochondrial $O_2^{\bullet-}$ in endothelial cells (BAEC) stimulated with the mitochondrial uncoupling agent antimycin A (AA). Extracellular $O_2^{\bullet-}$ was assessed by EPR signal inhibited by supplementation of 50 U/ml Mn-SOD (SOD).

to avoid interference with cellular $O_2^{\bullet-}$ detection. Cells were centrifuged and $O_2^{\bullet-}$ production was analysed in cell suspension [26]. Treatment of endothelial cells with the peroxynitrite donor SIN-1 significantly increased the production of cellular $O_2^{\bullet-}$ detected both by hydroxylamine probes and EMPO. The contribution of the eNOS uncoupling in $O_2^{\bullet-}$ production was estimated by decrease of nitroxide accumulation in the presence of eNOS inhibitor L-NAME (Figure 6) [26]. Treatment with SIN-1 resulted in increase of the intensity of the EPR signal: 2-fold for CAT1-H and EMPO, 2.5-fold for TM-H and TMT-H and 3-fold for PP-H (Figure 6, Table I). Supplementation of SIN-1-treated cells with Cu,Zn-SOD significantly reduced nitroxide accumulation, while addition of DMSO or uric acid did not affect oxidation of cyclic hydroxylamines. These data confirm that reaction of hydroxylamines with $O_2^{\bullet-}$ is a major source of accumulated nitroxide in endothelial cells.

Detection of $O_2^{\bullet-}$ in intact endothelial cells treated with antimycin A

Antimycin A stimulates the release of $O_2^{\bullet-}$ into the mitochondrial matrix and cellular cytoplasm [16]. It has been recently reported that nitrone spin traps fail to detect intracellular $O_2^{\bullet-}$ [16]. In this work we have investigated antimycin A-induced $O_2^{\bullet-}$ production in endothelial cells using hydroxylamine spin probes (Figure 7, Table I).

It was found that all spin probes detected $O_2^{\bullet-}$ in BAEC under basal conditions. Incubation of BAEC with CM-H and PP-H produced the strongest EPR signal and formation of corresponding nitroxides was only partially inhibited by extracellularly added Mn-SOD (50 U/ml). The amount of nitroxides formed due to reaction of $O_2^{\bullet-}$ with TM-H and TMT-H was 3-times less compared to CMH or PP-H.

Treatment of endothelial cells with antimycin A led to a major increase in CM-H oxidation rate, which was only partially suppressed by supplementation with extracellular Mn-SOD. Antimycin A caused a moderate increase in $O_2^{\bullet-}$-induced oxidation of TM-H and TMT-H. In contrast, oxidation of PP-H decreased in antimycin A-treated cells (Figure 7). Antimycin A inhibits ATP synthesis, thereby blocking all energy-dependent processes including active transport. This may prevent accumulation of PP-H inside antimycin A-treated cells and decrease the rate of oxidation of PP-H. A passive cellular diffusion of CM-H, TM-H and TMT-H was not likely affected by antimycin A supplementation and, thereby, antimycin A did not decrease the ability to scavenge intracellular $O_2^{\bullet-}$ by these probes.

Interestingly, detection of cellular $O_2^{\bullet-}$ in BAEC by cell-impermeable CAT1-H was completely blocked by supplementation with extracellular Mn-SOD both in basal conditions and upon stimulation with antimycin A (Figure 7, Table I), indicating that antimycin

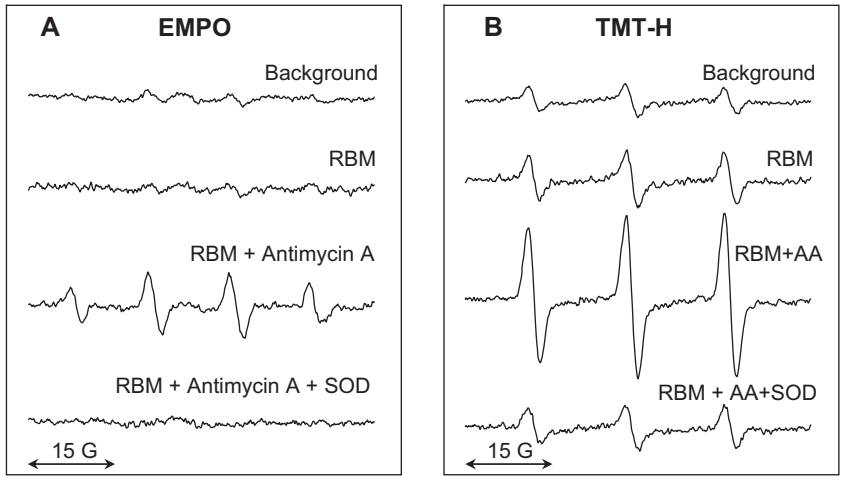

Figure 8. Detection of $O_2^{\bullet-}$ in the suspension of rat brain mitochondria (RBM). Superoxide radical production was measured in the samples containing RBM (0.5 mg/ml), 2 mM malate + 20 mM glutamate using spin trap EMPO (A) or cyclic hydroxylamine TMT-H (B) with or without antimycin A (AA).

A increased not only intracellular but also extracellular $O_2^{\bullet-}$ levels.

Detection of mitochondrial $O_2^{\bullet-}$ in isolated mitochondria

Small fractions of electrons in the mitochondrial respiratory chain can leak out and reduce oxygen, producing $O_2^{\bullet-}$ radicals [46]. Superoxide radicals formed on the inner membrane of the matrix are quickly dismutated by Mn-SOD and, therefore, cannot be detected outside of mitochondria, but can be estimated indirectly by leakage of H_2O_2 from mitochondria.

Superoxide produced on the outer membrane of the matrix can be released by mitochondria and detected as extramitochondrial $O_2^{\bullet-}$ [29]. Previously, succinate-dependent mitochondrial production of $O_2^{\bullet-}$ has been studied using DMPO and DEPMPO. In these experiments formation of the radical adducts was completely prevented by supplementation with extra-mitochondrial SOD [14,47]. However, identification of mitochondrial $O_2^{\bullet-}$ using spin trapping was complicated because of conversion of primary OOH-adduct into secondary OH-radical adduct by glutathione peroxidase and reduction of radical adducts [13–15]. Hydroxylamine spin probes can react with mitochondrial $O_2^{\bullet-}$ producing stable nitroxides which can be resistant to mitochondrial reduction. In this work we have investigated production of $O_2^{\bullet-}$ in isolated mitochondria under basal conditions and stimulated with antimycin A or rotenone using various hydroxylamine spin probes and EMPO.

No EMPO radical adducts formation was observed in rat brain mitochondria under basal conditions in the presence of malate+glutamate (Figure 8A). However, stimulation of mitochondrial $O_2^{\bullet-}$ production with antimycin A resulted in significant accumulation of EMPO/$^{\bullet}$OH radical adduct, which was completely blocked by supplementation with extra-mitochondrial SOD.

In contrast, TMT-H has been able to detect basal production of $O_2^{\bullet-}$ in rat brain mitochondria with malate+glutamate (Figure 8B, RBM vs background). Antimycin A further stimulated SOD-inhabitable accumulation of nitroxide (Figure 8B, RBM+AA vs RBM+AA+SOD). Interestingly, in antimycin A stimulated mitochondria TMT-H gave a twice higher EPR signal compared to EMPO (Figures 8A and B).

We have previously described the detection of $O_2^{\bullet-}$ in mitochondria using PP-H [29]. Indeed, supplementation of PP-H to isolated mitochondria resulted in significant accumulation of nitroxide which was further increased by antimycin A (Figure 9A). However, only a small fraction of the EPR signal was inhibited by SOD under basal conditions and PP-H showed a rather high background oxidation (Figure 9A).

We have recently found that CAT1-H is a very stable probe with minimal background oxidation [30]. Supplementation of CAT1-H to mitochondria resulted in accumulation of CAT1 nitroxide both in basal and antimycin A stimulated conditions (Figure 9B). These experiments showed that CAT1-H can be successfully used for detection of mitochondrial $O_2^{\bullet-}$ under

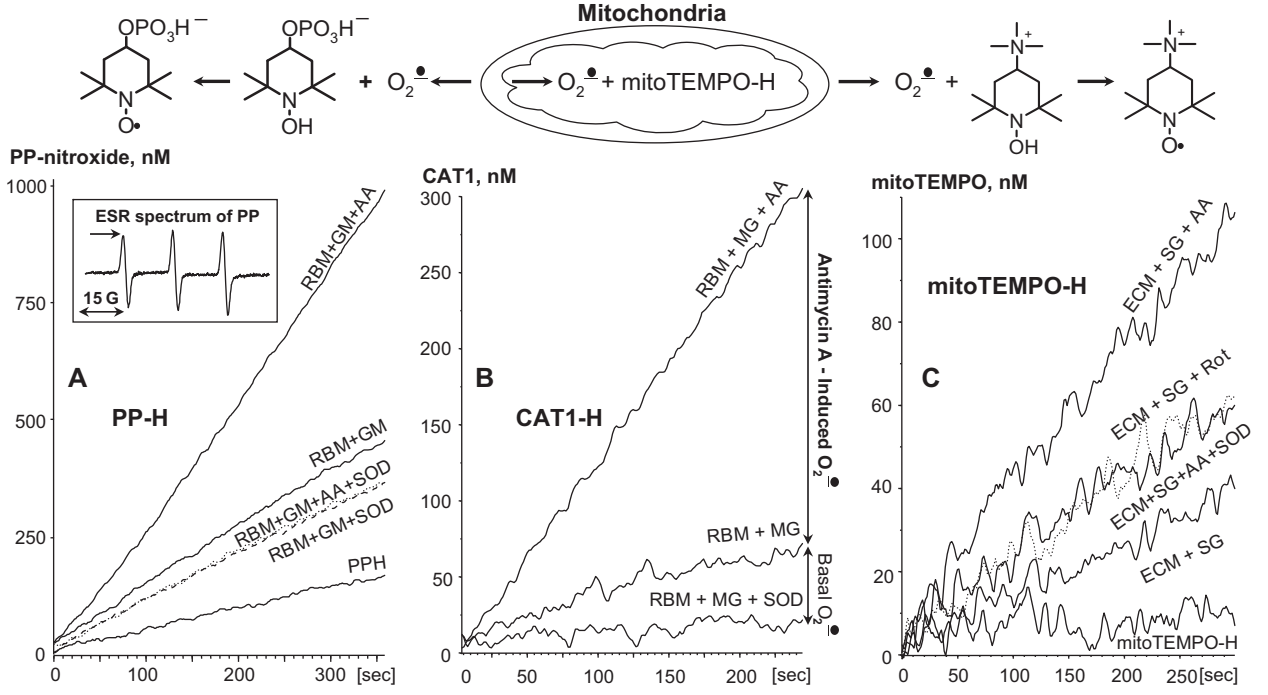

Figure 9. Detection of extramitochondrial $O_2^{\bullet-}$ in the suspension of rat brain mitochondria (RBM, 0.5 mg/ml) in the presence of malate (2 mM) and glutamate (20 mM) (MG); concentration of the hydroxylamine spin probes PP-H (A) or CAT1-H (B) was 0.5 mM. Mitochondrial matrix $O_2^{\bullet-}$ reacted with mitoTEMPO-H (C) in mitochondria isolated from bovine aortic endothelial cells (ECM) in the presence of succinate (10 mM) and glutamate (20 mM).

basal conditions as well as upon stimulation by antimycin A. The most important difference between PP-H and CAT1-H was observed in the detection of $O_2^{\bullet-}$ under basal conditions. Supplementation of SOD decreased the accumulation of CAT1 by a factor of 4 due to low background oxidation of CAT1-H, while PP-nitroxide signal was reduced only by 25%. It is interesting to note that antimycin A did not influence PP-nitroxide accumulation in the presence of SOD, indicating that intramitochondrial $O_2^{\bullet-}$ does not participate in PP-H oxidation. Thus, similarly to CAT1-H, PP-H does not penetrate mitochondria and detects only extramitochondrial $O_2^{\bullet-}$.

In order to measure $O_2^{\bullet-}$ production in a mitochondrial matrix we used mitochondria-targeted probe mitoTEMPO-H. Addition of mitochondria isolated from BAEC to mitoTEMPO-H significantly increased EPR signal (Figure 9C). Both rotenone and antimycin A further increased accumulation of nitroxide. As expected, supplementation of SOD did not affect rotenone-induced nitroxide accumulation and only partially attenuated the EPR signal, indicating that reaction with $O_2^{\bullet-}$ proceeds inside of the mitochondrial matrix.

Detection of intracellular and mitochondrial $O_2^{\bullet-}$ in intact cells

The above data indicate that that mitoTEMPO-H and CM-H can penetrate the cells and react with mitochondrial $O_2^{\bullet-}$ (Figures 4, 7 and 9). In contrast to CMH, mitochondria-targeted mitoTEMPO-H is actively accumulated in the mitochondrial matrix similar to other triphenylphosphonium cations [40], while CM-H may only passively diffuse across the lipid membrane. Another probe, CP-H, can permeate the cells, but it is mitochondria impermeable [48]. It is conceivable that specific intracellular localization of these spin probes will allow detection of $O_2^{\bullet-}$ in distinct cellular compartments: CP-H in the cytoplasm, mitoTEMPO-H in mitochondria, and CM-H in both compartments. In this work we have stimulated $O_2^{\bullet-}$ production in the cytoplasm with NADPH oxidases activator PMA while generation of $O_2^{\bullet-}$ in the mitochondrial matrix was induced by complex I inhibitor rotenone [29]. The site-specific production of $O_2^{\bullet-}$ in cytoplasm and mitochondria was investigated using 0.5 mM CP-H, 0.5 mM CM-H or 50 μM mitoTEMPO-H in intact human aortic endothelial cells (Figure 10) by EPR analysis of frozen samples [6]. In order to confirm detection of mitochondrial $O_2^{\bullet-}$ we used specific over-expression of the mitochondrial isoform of superoxide dismutase SOD2, while transfection of HAEC with GFP plasmid was used as a control.

Treatment of HAEC with PMA increased nitroxide accumulation in cells incubated with CP-H or CM-H but not with mitoTEMPO-H (Figures 10A–C). Stimulation of mitochondrial $O_2^{\bullet-}$ by rotenone increased nitroxide accumulation in cells incubated with CM-H or mitoTEMPO-H, but not with CP-H (Figures 10 A–C). Contribution of mitochondrial $O_2^{\bullet-}$ in EPR measurements of cellular $O_2^{\bullet-}$ was determined by a decrease of EPR signal in HAEC transfected with SOD2 plasmid compared to cells transfected with control GFP plasmid. EPR analysis of transfected HAEC showed that SOD2 over-expression did not affect measurements with CP-H (Figure 10D), but significantly attenuated measurements with CM-H and mitoTEMPO-H. Over-expression of mitochondrial SOD2 has significantly decreased detection of basal and rotenone-induced $O_2^{\bullet-}$ by CM-H or mitoTEMPO-H (Figures 10E and F).

Discussion

In this work we studied production of extracellular, intracellular and mitochondrial $O_2^{\bullet-}$ in neutrophils, cultured endothelial cells and isolated mitochondria using cyclic hydroxylamines of various lipophilicity and cell permeability. Despite significant differences in the chemical structures of cationic (CAT1-H), anionic (PP-H) and neutral (CM-H, TM-H, TMT-H) hydroxylamines show comparable rates of oxidation with $O_2^{\bullet-}$ in the cell-free xanthine oxidase system, which are significantly higher than the rate of accumulation of the EMPO/$^{\bullet}$OOH radical adduct. The performance of different hydroxylamine spin probes in cellular systems, however, strongly depend on differences in lipophylicity, cell permeability and propensity to specific active transport.

All cationic, anionic and neutral spin probes showed similar results in detection of $O_2^{\bullet-}$ in the cell-free xanthine oxidase system (Figure 2) and measurements of extracellular $O_2^{\bullet-}$ produced by PMA-stimulated neutrophils (Figure 5, Table I). Meanwhile, detection of intracellular $O_2^{\bullet-}$ was very distinct (Figures 7 and 10). Thus, the efficacy of intracellular $O_2^{\bullet-}$ detection is determined not only by chemical reactivity of the spin probes, but also by lipophility (Table I, K_p), cell permeability (Figure 4) and sub-cellular distribution of these compounds (Figure 11). The presence of cationic group (CAT1-H), carrier or targeting groups such as phosphate or lipophilic triphenylphosphonium cation was particularly important for probe subcellular distribution and site-specific $O_2^{\bullet-}$ detection.

All the spin probes showed accumulation of nitroxides in the suspension of BAEC both in basal conditions and upon stimulation with peroxynitrite, but in these experiments cell-impermeable CAT1-H showed the lowest oxidation rate and only CAT1 nitroxide accumulation was completely inhibited by extracellular SOD (Figures 7 and 11). In contrast, formation of nitroxides from cell-permeable hydroxylamines CM-H, PP-H, TM-H and TMT-H was only partially suppressed by extracellular SOD (Figures 6, 7 and 11).

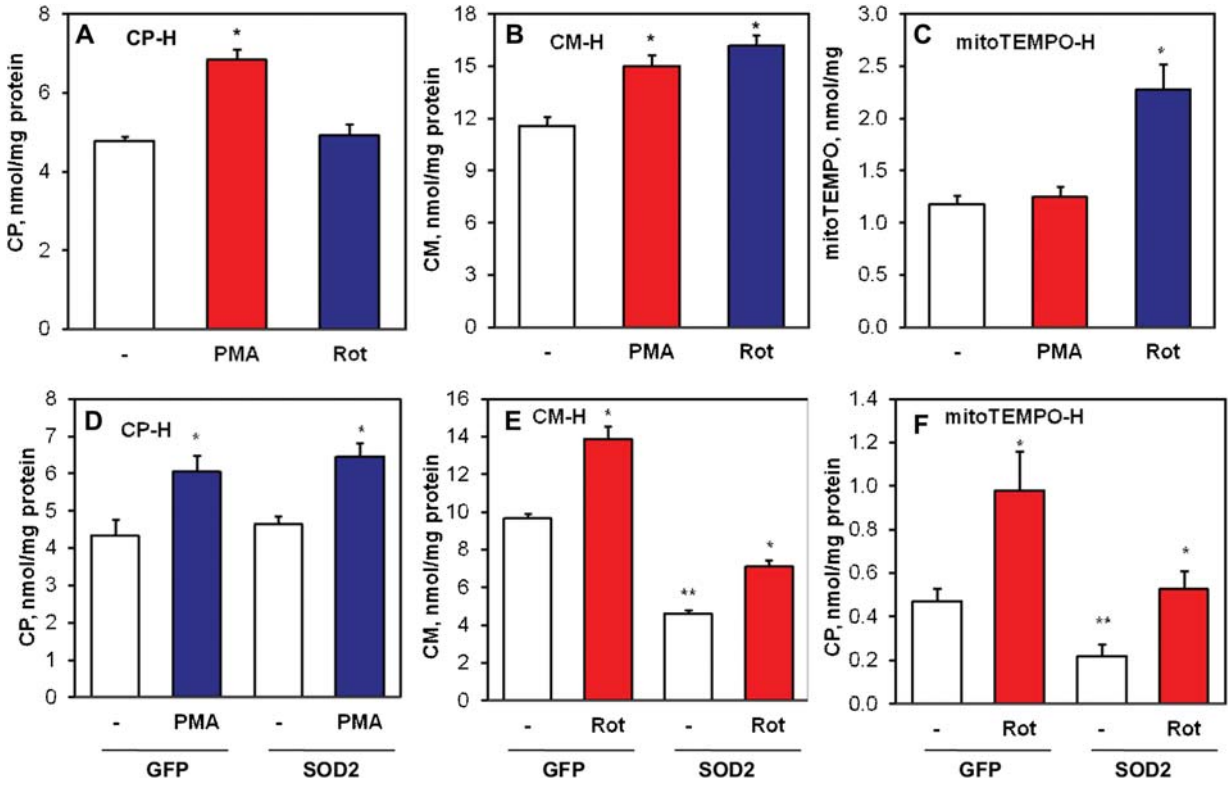

Figure 10. EPR detection of intracellular and mitochondrial $O_2^{\bullet-}$ in intact human aortic endothelial cells (HAEC). Production of intracellular $O_2^{\bullet-}$ was stimulated with PMA (5 μM, 30 min). Generation of mitochondrial $O_2^{\bullet-}$ was induced by rotenone (5 μM, 30 min). Following treatment with PMA, rotenone or DMSO as a vehicle, HAEC were incubated with 0.5 mM spin probes for 20 min at 37°C. Then cells were collected and into a 1-ml syringe with 0.6 ml buffer and snap-frozen in liquid nitrogen. Samples were analysed in a finger Dewar filled with liquid nitrogen. Production of $O_2^{\bullet-}$ in intact non-transfected HAEC was measured in using cell permeable spin probe CPH (A), mitochondria permeable CMH (B) or mitochondria-targeted mitoTEMPO-H (C). Contribution of mitochondrial $O_2^{\bullet-}$ in EPR measurements of cellular $O_2^{\bullet-}$ was determined by inhibition of EPR signal in HAEC transfected with SOD2 plasmid compared transfection with control GFP plasmid. Analysis of transfected HAEC showed that SOD2 over-expression did not affect measurements with CPH (D), but significantly attenuated measurements with CMH (E) and mitoTEMPO-H (F).

Differences in cell-permeable spin probes behaviour in the presence of BAEC and neutrophils coincides with the previously known facts about extracellular $O_2^{\bullet-}$ production by neutrophils and intracellular location of eNOS in BAEC. Thus, supplementation of cell-permeable hydroxylamines with extracellular SOD may provide a simple method to differentiate intracellular and extracellular $O_2^{\bullet-}$. Moreover, quantification of both extracellular and intracellular $O_2^{\bullet-}$ production is possible (Figure 11).

Detection of intracellular $O_2^{\bullet-}$ correlates with accumulation of the spin probes inside cells. CM-H showed very strong cellular accumulation and the highest rate of intracellular nitroxide formation among all tested hydroxylamines (Figures 4–7). It is interesting to note that anionic PP-H demonstrated higher sensitivity in the detection of endothelial $O_2^{\bullet-}$ than cationic CAT1-H. The phosphate-containing probe PP-H was found to accumulate inside cells, presumably via active transport. Recently, we have validated the detection of extracellular $O_2^{\bullet-}$ in intact tissues using CAT1-H [30] and found it extremely useful, particularly due to resistance to auto-oxidation. Here we successfully applied CAT1-H to study the release of $O_2^{\bullet-}$ by mitochondria. Our data suggest that CAT1-H is an optimal probe for $O_2^{\bullet-}$ quantification in sub-cellular fractions and in cell-free samples.

Application of neutral cell permeable hydroxylamines (CM-H, TM-H, TMT-H) showed a 3-fold increase in intracellular $O_2^{\bullet-}$ production by endothelial cells treated with antimycin A, while cell impermeable CAT1-H showed only a 30% increase in the extracellular $O_2^{\bullet-}$. These data suggest that only a small fraction of mitochondrial $O_2^{\bullet-}$ released into the cytoplasm is likely to escape from the cell and react with extracellular probes (Figure 7, CM-H vs CAT1-H). Experiments with peroxynitrite-treated BAEC showed that the extracellular fraction of $O_2^{\bullet-}$ produced by uncoupled eNOS is higher than that from the mitochondrial source. This difference may result from eNOS localization in caveolae associated with extracellular membrane [49]. As a consequence, localization of the $O_2^{\bullet-}$ sources in the proximity to extracellular membranes greatly increases the probability for $O_2^{\bullet-}$ release out of the cell. Therefore, it is likely that extracellular $O_2^{\bullet-}$ detection strongly depends on the sources of cellular $O_2^{\bullet-}$, due to differences in their intracellular localization. This may represent an additional challenge in

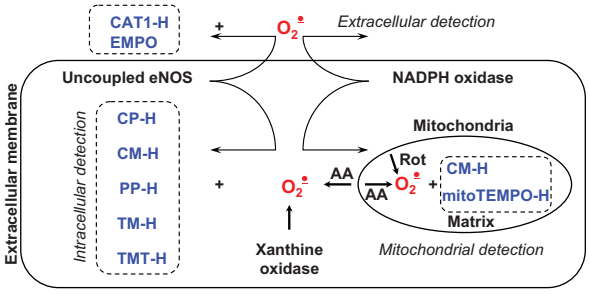

Figure 11. General scheme of EPR detection of superoxide in extracellular, intracellular or mitochondrial compartments using cyclic hydroxylamine spin probes.

the analysis of intracellular $O_2^{\bullet-}$ using extracellular detection by spin traps or cytochrome c [6] because a minor change in extracellular $O_2^{\bullet-}$ may correspond to a several-fold increase in local intracellular $O_2^{\bullet-}$. The results of extracellular $O_2^{\bullet-}$ detection, therefore, should be interpreted with caution. Cell-permeable hydroxylamine spin probes described in this work may provide a useful tool for investigation of sources of intracellular $O_2^{\bullet-}$ (Figure 11).

A number of mitochondria-targeted nitrone spin traps have been designed to accumulate in mitochondria and to detect free radicals generated in the matrix [50]. Spin trapping in mitochondria, however, required very a high concentration of mito-DEPMPO (50 mM) and supplementation with SOD completely abolished the EPR signal to the level of oxygen-free mitochondria [46], indicating detection of extra-mitochondrial $O_2^{\bullet-}$ only. Our experiments with SOD2 over-expressed HAEC showed that both mitoTEMPO-H and CM-H can detect mitochondrial $O_2^{\bullet-}$. Mitochondria-targeted accumulation of mitoTEMPO-H allowed specific $O_2^{\bullet-}$ detection in mitochondria while CM-H measured $O_2^{\bullet-}$ both in the cytoplasm and mitochondria (Figure 11). In contrast, mitochondria-impermeable CP-H showed PMA-stimulated $O_2^{\bullet-}$ production in the cytoplasm but did not detect rotenone-induced mitochondrial $O_2^{\bullet-}$.

Cyclic hydroxylamine probes react with $O_2^{\bullet-}$ much faster ($k \sim 10^3$–10^4 $M^{-1}s^{-1}$, pH = 7.4) than nitrone spin traps ($k \sim 35$–75 $M^{-1}s^{-1}$, pH = 7.4) and can compete with cellular antioxidants for reaction with intracellular $O_2^{\bullet-}$ [11]. Furthermore, cyclic hydroxylamine probes showed a relatively slow decrease in nitroxide accumulation rate in the reaction with superoxide while the nitrone spin trap showed a much higher deviation from linear accumulation of radical adduct (Figure 2 and Dikalov et al. [51]), presumably due to bimolecular decay of the radical adduct which is typical for β–proton containing nitroxides. Therefore, hydroxylamine spin probes represent a very useful tool for quantitative analysis of cellular $O_2^{\bullet-}$.

In spite of the obvious advantage of using cyclic hydroxylamines for $O_2^{\bullet-}$ quantification, this particular approach reveals certain limitations. The first is the scarcity of spectral information, because the product of oxidation has the same three-line EPR signal regardless of species responsible for oxidation. However, the simplicity of the EPR spectrum results in a higher signal-to-noise ratio due to distribution of EPR intensity between three lines for nitroxides instead of six lines for radical adducts, and provides easy analysis both in liquid and frozen samples. The second potential limitation is the non-specific oxidation by transition metal ions (Cu^{2+}, Fe^{3+}) and some heme proteins. Stability of hydroxylamines towards background oxidation can be enhanced by supplementation of chelating agents (DTPA, deferoxamine, DETC). In addition, we also found that six-membered ring hydroxylamines, such as CAT1-H, TM-H and TMT-H, have lower levels of background EPR signal compared to five-membered probes (CP-H, CM-H). The third limitation is the lack of specificity in $O_2^{\bullet-}$ detection. The lack of specificity of cyclic hydroxylamines can be overcome by the use of SOD and inhibitors of sources of $O_2^{\bullet-}$ production, such as NADPH oxidase, xanthine oxidase or mitochondria [33], while reaction with peroxynitrite can be inhibited by uric acid [26]. We have found that SOD inhibits 70–98% of nitroxide production [19,31], while acute addition of uric acid did not show a significant effect. These data suggests that $O_2^{\bullet-}$ represents a major pull of free radicals produced in cells and tissue. Overall, hydroxylamine probes will not replace spin traps, but they provide a new useful tool for EPR detection of cellular $O_2^{\bullet-}$.

The above-described examples demonstrate that a new set of hydroxylamine spin probes allows site-specific detection of cellular and mitochondrial $O_2^{\bullet-}$. The main advantage of hydroxylamine spin probes is variability of chemical structure. The use of this variability permits molecular design of specific probes 'targeted' to certain cellular compartment and the combination of several hydroxylamine spin probes may provide unique information about location of radical production, which can hardly be obtained using other methods.

Acknowledgement

Authors are grateful to Dr Maziar Zafari for his help in editing the manuscript.

Declaration of interest

This research was supported by NIH grants PO-1 HL058000-05, PO-1 HL075209.

References

[1] McCord JM, Fridovich I. The biology and pathology of oxygen radicals. Ann Intern Med 1978;89:122–127.

[2] Singh A. Chemical and biochemical aspects of superoxide radicals and related species of activated oxygen. Can J Physiol Pharmacol 1982;60:1330–1345.
[3] Griendling KK, Sorescu D, Lassegue B, Ushio-Fukai M. Modulation of protein kinase activity and gene expression by reactive oxygen species and their role in vascular physiology and pathophysiology. Arterioscler Thromb Vasc Biol 2000; 20:2175–2183.
[4] Wolin MS, Gupte SA, Oeckler RA. Superoxide in the vascular system. J Vasc Res 2002;39:191–207.
[5] Griendling KK, Sorescu D, Ushio-Fukai M. NAD(P)H oxidase: role in cardiovascular biology and disease. Circ Res 2000;86:494–501.
[6] Dikalov S, Griendling KK, Harrison DG. Measurement of reactive oxygen species in cardiovascular studies. Hypertension 2007;49:717–727.
[7] Wolin MS, Ahmad M, Gupte SA. The sources of oxidative stress in the vessel wall. Kidney Int 2005;67:1659–1661.
[8] Vasquez-Vivar J, Hogg N, Pritchard KA, Jr, Martasek P, Kalyanaraman B. Superoxide anion formation from lucigenin: an electron spin resonance spin-trapping study. FEBS Lett 1997;403:127–130.
[9] Tsai P, Ichikawa K, Mailer C, Pou S, Halpern HJ, Robinson BH, Nielsen R, Rosen GM. Esters of 5-carboxyl-5-methyl-1-pyrroline n-oxide: a family of spin traps for superoxide. J Org Chem. 2003;68:7811–7817.
[10] Frejaville C, Karoui H, Tuccio B, Le Moigne F, Culcasi M, Pietri S, Lauricella R, Tordo P. 5-(diethoxyphosphoryl)-5-methyl-1-pyrroline n-oxide: a new efficient phosphorylated nitrone for the *in vitro* and *in vivo* spin trapping of oxygen-centered radicals. J Med Chem 1995;38:258–265.
[11] Dikalov SI, Dikalova AE, Mason RP. Noninvasive diagnostic tool for inflammation-induced oxidative stress using electron spin resonance spectroscopy and an extracellular cyclic hydroxylamine. Arch Biochem Biophys 2002;402:218–226.
[12] Dikalov S, Khramtsov V, Zimmer G. Determination of rate constants of the reactions of thiols with superoxide radical by electron paramagnetic resonance: critical remarks on spectrophotometric approaches. Arch Biochem Biophys 1996; 326:207–218.
[13] Dikalov S, Landmesser U, Harrison DG. Geldanamycin leads to superoxide formation by enzymatic and non-enzymatic redox cycling. Implications for studies of Hsp90 and endothelial cell nitric-oxide synthase. J Biol Chem 2002;277: 25480–25485.
[14] Zwicker K, Dikalov S, Matuschka S, Mainka L, Hofmann M, Khramtsov V, Zimmer G. Oxygen radical generation and enzymatic properties of mitochondria in hypoxia/reoxygenation. Arzneimittelforschung 1998;48:629–636.
[15] Culcasi M, Rockenbauer A, Mercier A, Clement JL, Pietri S. The line asymmetry of electron spin resonance spectra as a tool to determine the cis:trans ratio for spin-trapping adducts of chiral pyrrolines N-oxides: the mechanism of formation of hydroxyl radical adducts of EMPO, DEPMPO, and DIPPMPO in the ischemic-reperfused rat liver. Free Radic Biol Med 2006;40:1524–1538.
[16] Zhao H, Joseph J, Fales HM, Sokoloski EA, Levine RL, Vasquez-Vivar J, Kalyanaraman B. Detection and characterization of the product of hydroethidine and intracellular superoxide by HPLC and limitations of fluorescence. Proc Natl Acad Sci USA. 2005;102:5727–5732.
[17] Zielonka J, Zhao H, Xu Y, Kalyanaraman B. Mechanistic similarities between oxidation of hydroethidine by fremy's salt and superoxide: stopped-flow optical and EPR studies. Free Radic Biol Med 2005;39:853–863.
[18] Fernandes DC, Wosniak J, Jr, Pescatore LA, Bertoline MA, Liberman M, Laurindo FR, Santos CX. Analysis of dhe-derived oxidation products by hplc in the assessment of superoxide production and nadph oxidase activity in vascular systems. Am J Physiol Cell Physiol 2007;292:413–422.
[19] Dikalova A, Clempus R, Lassegue B, Cheng G, McCoy J, Dikalov S, San Martin A, Lyle A, Weber DS, Weiss D, Taylor WR, Schmidt HH, Owens GK, Lambeth JD, Griendling KK. Nox1 overexpression potentiates angiotensin II-induced hypertension and vascular smooth muscle hypertrophy in transgenic mice. Circulation 2005;112:2668–2676.
[20] Dikalov S, Fink B, Skatchkov M, Bassenge E. Comparison of glyceryl trinitrate-induced with pentaerythrityl tetranitrate-induced *in vivo* formation of superoxide radicals: effect of vitamin c. Free Radic Biol Med 1999;27:170–176.
[21] Marchesi E, Rota C, Fann YC, Chignell CF, Mason RP. Photoreduction of the fluorescent dye 2'-7'-dichlorofluorescein: a spin trapping and direct electron spin resonance study with implications for oxidative stress measurements. Free Radic Biol Med 1999;26:148–161.
[22] Goldstein S, Merenyi G, Russo A, Samuni A. The role of oxoammonium cation in the sod-mimic activity of cyclic nitroxides. J Am Chem Soc 2003;125:789–795.
[23] Dikalov S, Skatchkov M, Bassenge E. Spin trapping of superoxide radicals and peroxynitrite by 1-hydroxy-3-carboxy-pyrrolidine and 1-hydroxy-2,2,6, 6-tetramethyl-4-oxo-piperidine and the stability of corresponding nitroxyl radicals towards biological reductants. Biochem Biophys Res Commun 1997; 231:701–704.
[24] Dikalov S, Skatchkov M, Fink B, Bassenge E. Quantification of superoxide radicals and peroxynitrite in vascular cells using oxidation of sterically hindered hydroxylamines and electron spin resonance. Nitric Oxide 1997;1:423–431.
[25] Kuzkaya N, Weissmann N, Harrison DG, Dikalov S. Interactions of peroxynitrite, tetrahydrobiopterin, ascorbic acid, and thiols: implications for uncoupling endothelial nitric-oxide synthase. J Biol Chem 2003;278:22546–22554.
[26] Kuzkaya N, Weissmann N, Harrison DG, Dikalov S. Interactions of peroxynitrite with uric acid in the presence of ascorbate and thiols: implications for uncoupling endothelial nitric oxide synthase. Biochem Pharmacol 2005;70:343–354.
[27] Wyche KE, Wang SS, Griendling KK, Dikalov SI, Austin H, Rao S, Fink B, Harrison DG, Zafari AM. C242t cyba polymorphism of the nadph oxidase is associated with reduced respiratory burst in human neutrophils. Hypertension 2004; 43:1246–1251.
[28] Dikalov S, Grigor'ev IA, Voinov M, Bassenge E. Detection of superoxide radicals and peroxynitrite by 1-hydroxy-4-phosphonooxy-2,2,6,6-tetramethylpiperidine: quantification of extracellular superoxide radicals formation. Biochem Biophys Res Commun 1998;248:211–215.
[29] Panov A, Dikalov S, Shalbuyeva N, Taylor G, Sherer T, Greenamyre JT. Rotenone model of parkinson disease: multiple brain mitochondria dysfunctions after short term systemic rotenone intoxication. J Biol Chem 2005;280: 42026–42035.
[30] Gongora MC, Qin Z, Laude K, Kim HW, McCann L, Folz JR, Dikalov S, Fukai T, Harrison DG. Role of extracellular superoxide dismutase in hypertension. Hypertension 2006;48:473–481.
[31] Hanna IR, Hilenski LL, Dikalova A, Taniyama Y, Dikalov S, Lyle A, Quinn MT, Lassegue B, Griendling KK. Functional association of nox1 with p22phox in vascular smooth muscle cells. Free Radic Biol Med 2004;37:1542–1549.
[32] McNally JS, Davis ME, Giddens DP, Saha A, Hwang J, Dikalov S, Jo H, Harrison DG. Role of xanthine oxidoreductase and NAD(P)H oxidase in endothelial superoxide production in response to oscillatory shear stress. Am J Physiol Heart Circ Physiol 2003;285:2290–2297.
[33] Fraticelli A, Serrano CV, Jr, Bochner BS, Capogrossi MC, Zweier JL. Hydrogen peroxide and superoxide modulate leukocyte adhesion molecule expression and leukocyte endothelial adhesion. Biochim Biophys Acta 1996;1310:251–259.
[34] Sims NR. Rapid isolation of metabolically active mitochondria from rat brain and subregions using percoll density gradient centrifugation. J Neurochem 1990;55:698–707.

[35] Trounce IA, Kim YL, Jun AS, Wallace DC. Assessment of mitochondrial oxidative phosphorylation in patient muscle biopsies, lymphoblasts, and transmitochondrial cell lines. Methods Enzymol 1996;264:484–509.

[36] Panov AV, Lund S, Greenamyre JT. Ca^{2+}-induced permeability transition in human lymphoblastoid cell mitochondria from normal and huntington's disease individuals. Mol Cell Biochem 2005;269:143–152.

[37] Dikalov S, Jiang J, Mason RP. Characterization of the high-resolution esr spectra of superoxide radical adducts of 5-(diethoxyphosphoryl)-5-methyl-1-pyrroline n-oxide (DEPMPO) and 5,5-dimethyl-1-pyrroline n-oxide (DMPO). Analysis of conformational exchange. Free Radic Res 2005;39:825–836.

[38] Itoh O, Aoyama M, Yokoyama H, Obara H, Ohya-Nishiguchi H, Kamada H. Sensitive ESR determination of intracellular oxidative stress by using acyl-protected hydroxylamines as new spin reagents. Chem Lett 2000;29:304–305.

[39] Rosen GM, Finkelstein E, Rauckman EJ. A method for the detection of superoxide in biological systems. Arch Biochem Biophys. 1982;215:367–378.

[40] Israeli A, Patt M, Oron M, Samuni A, Kohen R, Goldstein S. Kinetics and mechanism of the comproportionation reaction between oxoammonium cation and hydroxylamine derived from cyclic nitroxides. Free Radic Biol Med. 2005;38:317–324.

[41] Murphy MP, Smith RA. Targeting antioxidants to mitochondria by conjugation to lipophilic cations. Annu Rev Pharmacol Toxicol 2007;47:629–656.

[42] Glinn M, Ni B, Paul SM. Characterization of Na(+)-dependent phosphate uptake in cultured fetal rat cortical neurons. J Neurochem 1995;65:2358–2365.

[43] Laursen JB, Somers M, Kurz S, McCann L, Warnholtz A, Freeman BA, Tarpey M, Fukai T, Harrison DG. Endothelial regulation of vasomotion in apoE-deficient mice: implications for interactions between peroxynitrite and tetrahydrobiopterin. Circulation 2001;103:1282–1288.

This paper was first published online on Early Online on 9 December 2010.

[44] Landmesser U, Dikalov S, Price SR, McCann L, Fukai T, Holland SM, Mitch WE, Harrison DG. Oxidation of tetrahydrobiopterin leads to uncoupling of endothelial cell nitric oxide synthase in hypertension. J Clin Invest 2003;111:1201–1209.

[45] Xia Y, Dawson VL, Dawson TM, Snyder SH, Zweier JL. Nitric oxide synthase generates superoxide and nitric oxide in arginine-depleted cells leading to peroxynitrite-mediated cellular injury. Proc Natl Acad Sci USA 1996;93:6770–6774.

[46] Staniek K, Gille L, Kozlov AV, Nohl H. Mitochondrial superoxide radical formation is controlled by electron bifurcation to the high and low potential pathways. Free Radic Res 2002;36:381–387.

[47] Hardy M, Rockenbauer A, Vasquez-Vivar J, Felix C, Lopez M, Srinivasan S, Avadhani N, Tordo P, Kalyanaraman B. Detection, characterization, and decay kinetics of ROS and thiyl adducts of mito-DEPMPO spin trap. Chem Res Toxicol 2007;20:1053–1060.

[48] Dhanasekaran A, Kotamraju S, Karunakaran C, Kalivendi SV, Thomas S, Joseph J, Kalyanaraman B. Mitochondria superoxide dismutase mimetic inhibits peroxide-induced oxidative damage and apoptosis: role of mitochondrial superoxide. Free Radic Biol Med 2005;39:567–583.

[49] Li L, Haynes MP, Bender JR. Plasma membrane localization and function of the estrogen receptor alpha variant (ER46) in human endothelial cells. Proc Natl Acad Sci USA 2003;100:4807–4812.

[50] El Fangour S, Marini M, Good J, McQuaker SJ, Shiels PG, Hartley RC. Nitrones for understanding and ameliorating the oxidative stress associated with aging. Age (Dordr) 2009;31:269–276.

[51] Dikalov SI, Li W, Mehranpour P, Wang SS, Zafari AM. Production of extracellular superoxide by human lymphoblast cell lines: comparison of electron spin resonance techniques and cytochrome C reduction assay. Biochem Pharmacol 2007;73:972–980.